CrystEngComm

RSC Publishing

PAPER

View Article Online
View Journal | View Issue

Cite this: *CrystEngComm*, 2013, **15**, 4684

Improved synthesis and crystal structure of the flexible pillared layer porous coordination polymer: Ni(1,2-bis(4-pyridyl)ethylene)[Ni(CN)$_4$]†

W. Wong-Ng,[a] J. T. Culp,[bc] Y. S. Chen,[d] P. Zavalij,[e] L. Espinal,[a] D. W. Siderius,[a] A. J. Allen,[a] S. Scheins[d] and C. Matranga[b]

Received 6th January 2013,
Accepted 3rd April 2013

DOI: 10.1039/c3ce00017f

www.rsc.org/crystengcomm

This paper reports our synthesis of flexible coordination polymer, Ni(L)[Ni(CN)$_4$], (L = 1,2-bis(4-pyridyl)ethylene (nicknamed bpene)), and its structural characterization using synchrotron single crystal X-ray diffraction. The structure of the purplish crystals has been determined to be monoclinic, space group $P2_1/m$, a = 13.5941(12) Å, b = 14.3621(12) Å, c = 14.2561(12) Å, β = 96.141(2)°, V = 2767.4(4) Å^3, Z = 4, D_c = 1.46 g cm^{-1}. Ni(bpene)[Ni(CN)$_4$] assumes a pillared layer structure with layers defined by Ni[Ni(CN)$_4$]$_n$ nets and bpene ligands acting as pillars. With the present crystallization technique which involves the use of concentrated ammonium hydroxide solution and dimethyl sulfoxide (DMSO), disordered free bpene ligands and solvents of crystallization (DMSO and water molecules) occupy the pores, resulting in a formula of Ni(bpene)[Ni(CN)$_4$]·½bpene·DMSO·2H$_2$O, or Ni$_2$N$_7$C$_{24}$H$_{25}$SO$_3$. Without the inclusion of free bpene ligands and solvent molecules, the free volume is approximately 61% of the total volume; this free volume fraction is reduced to 50% with the free ligands present. Pores without the free ligands were found to have a local diameter of 5.7 Å and a main aperture of 3.5 Å. Based on the successful crystal synthesis, we also devised a new bulk synthetic technique which yielded a polycrystalline material with a significantly improved CO_2 uptake as compared to the originally reported powder material. The improved synthetic technique yielded a polycrystalline material with 40% higher CO_2 uptake compared to the previously reported powder material. An estimated 14.4 molecules of CO_2 per unit cell was obtained.

Introduction

Fossil fuels will remain a major global energy source for the foreseeable future. Given current widespread concern over the associated carbon dioxide emission, significant advances in carbon capture and storage technology will be crucial for ensuring the sustainability of this energy supply.[1] The potential for porous coordination polymers (PCPs, commonly referred to as metal–organic frameworks, or MOFs)[2] to become commercially important for novel areas such as molecular sorption, sensing and gas storage applications is now widely recognized.[3] The majority of MOF materials reported to date have been found to exhibit insignificant structural changes during guest exchange. In recent years, however, a number of interesting compounds known as flexible porous coordination polymers (or flexible MOFs) have been discovered which show reversible structural transitions between low porosity and high porosity phases during the adsorption and desorption of guests.[4]

Development of novel solid sorbent materials could provide a cost-effective way to capture CO_2. In particular, PCPs consisting of pillared layer structures have been widely pursued as a route to rationally designed architectures.[5] Within the family of pillared layer PCPs, the Hofmann compounds [M′(L)M(CN)$_4$]$_n$ (M = Fe, Ni, Zn, or Cd; M′ = Ni, Pd, or Pt; L = pillar ligand)[6] have been shown to be especially diverse.[7–11] These materials are characterized by the presence of square planar [M(CN)$_4$]$^{2-}$ complexes bridged into extended 2-D networks *via* M–CN–M′ linkages. The octahedral coordination sphere of the M′ site is completed through complexation of a bidentate pillar ligand which results in the growth of a three-dimensional network. The absence of coordinated pillar ligands on the square planar M sites results in the formation of open pore structures. Using this structural motif, a wide

[a]*Material Measurement Laboratory, National Institute of Standards and Technology, Gaithersburg, MD 20899, USA*
[b]*National Energy Technology Laboratory, United States Department of Energy, P. O. Box 10940, Pittsburgh, PA 15236, USA*
[c]*URS Corporation, South Park, PA 15219, USA*
[d]*ChemMatCARS, University of Chicago, Argonne, IL 60439, USA*
[e]*Department of Chemistry and Biochemistry, University of Maryland, College Park, MD 20742, USA*

† Electronic supplementary information (ESI) available: Description of crystallography, supplementary figures, including detailed atomic labeling, disordered ligands, powder XRD profiles, table of bond parameters, CIF file for the flexible MOF reported in this paper. CCDC 915487. For ESI and crystallographic data in CIF or other electronic format see DOI: 10.1039/c3ce00017f

range of materials can be created through substitution of the octahedral metal sites and/or pillar ligands.[8] The tailorability of these materials renders them well-suited for studying the effects of pore size on gas adsorption behavior.[8] Derivatives with Fe(II) in the octahedral sites have also been widely studied for their interesting and often guest-dependent spin crossover behavior.[10,11]

Materials based on the pillared cyano-bridged architecture can be structurally rigid or dynamic depending on the choice of pillar ligands.[9] Flexible MOFs change their structures upon adsorption and desorption of CO_2, resulting in dramatic effects on their adsorption and desorption isotherms. Our present study concerns a flexible derivative of $Ni(L)[Ni(CN)_4]_n$, where L is the pillar ligand 1,2-bis(4-pyridyl)ethylene, nicknamed 'bpene' (Fig. 1), which has an ideal formula of $Ni_2N_6C_{16}H_{10}$. This material has been recently shown to exhibit unusual guest-dependent adsorption and desorption behavior for CO_2 and N_2 characteristic of a flexible PCP where there is only minimal adsorption below a threshold or 'gate-opening' pressure, above which significant gas adsorption takes place. The desorption isotherms differ from the adsorption isotherms, yielding hysteresis loops.[8] While extensive characterizations have been performed on $Ni(bpene)[Ni(CN)_4]$ in powder form, a full structural analysis of the material until now has not been possible due to the difficulty of obtaining isolated single crystals of the material.

In order to understand the CO_2 sorption mechanism of $Ni(bpene)[Ni(CN)_4]$, a detailed crystal structure analysis is necessary. Crystal structures of most members of the $Ni(L)[Ni(CN)_4]$ family of compounds, however, have remained elusive mainly due to the difficulty of obtaining quality single crystals of these insoluble polymeric materials. Structural analyses of these materials can be further complicated by the propensity of these materials to be obtained as twinned crystals with disordered ligands and guests. In an effort to overcome these analytical barriers, a novel crystallization technique was developed. In addition, the use of synchrotron X-rays allowed the structural analysis to be conducted on micron-sized crystals which greatly minimized complications associated with crystal twinning. This paper reports our synthesis of crystalline $Ni(bpene)[Ni(CN)_4]$, and its structural characterization using the synchrotron X-ray facility at the ChemMatCARS. Based on the successful single crystal synthesis, we also devised a new bulk synthetic technique which yielded a polycrystalline material with a significantly improved CO_2 uptake as compared to the originally reported powder material.

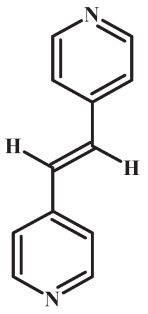

Fig. 1 Schematic drawing of the bpene ligand, $C_{16}H_{10}N_6Ni_2$.

Experimental[12]

Synthesis/crystal growth

A 35 mL 19/22 flask was charged with 0.5 mmol (0.136 g) polymeric nickel cyanide hydrate $Ni[Ni(CN)_4]_n(H_2O)_3$ and made to dissolve through the sequential addition of 5 mL H_2O, 5 mL concentrated ammonium hydroxide solution (~28%), and 5 mL dimethyl sulfoxide (DMSO) with stirring. (**Caution:** do not mix concentrated ammonium hydroxide and DMSO directly as rapid outgassing of NH_3 can occur.) A solution of 0.75 mmol (0.136 g) of 1,2-bis(4-pyridyl)ethylene "bpene" in 10 mL DMSO was then added to the resulting solution. A six inch air-cooled condenser was added and the flask was transferred to an oil bath preheated to 70 °C. The temperature of the oil bath was ramped to 90 °C over approximately 30 minutes after which the stirring was stopped and the reaction left at 90 °C undisturbed for 24 h to 48 h. The dissolved NH_3 bubbled out of the solution rapidly during the initial hour with the simultaneous formation of a small amount of finely powdered precipitate, then slowed significantly while a crystalline product formed over the next several hours. After completion, the reaction mixture was cooled to room temperature and the resulting violet crystals were isolated by pipetting off the majority of a fine particle suspension of impurities while being careful to leave the crystals wetted within the reaction mixture. The impurities were removed by filtration and the filtrate returned to the flask. The pipetting and filtration cycle was repeated until the powdered impurities were removed. The light violet crystals were kept stored in the cleaned reaction mixture in a capped vial at room temperature until the X-ray diffraction measurements were taken.

Polycrystalline $Ni(bpene)[Ni(CN)_4]$ (improved synthesis)

An improved synthesis of polycrystalline $Ni(bpene)[Ni(CN)_4]$ as compared to the procedure described[8] is as follows. A flask was charged with 4 mmol of polymeric $Ni[Ni(CN)_4]_n$ hydrate. The solid was dissolved at room temperature with stirring by sequential addition of 15 mL of H_2O, 15 mL of concentrated ammonium hydroxide solution (~28%), and 15 mL of DMSO. (**Caution:** do not mix concentrated ammonium hydroxide and DMSO directly as rapid outgassing of NH_3 can occur.) To the clear solution was added 5.6 mmol of 1,2-bis(4-pyridyl)ethylene dissolved in 35 mL of DMSO. The pressure in the flask was slowly decreased over time using a water aspirator to outgas the NH_3 at a controlled and relatively constant rate which was slow enough to prevent excessive bubbling. After approximately 90 minutes, the precipitated solid was filtered off and washed with a 1 : 3 H_2O : DMSO mixture, followed by acetone. The solid was then extracted in 100 mL of acetone at reflux for 2 hours and isolated by filtration. (Extracted bpene

ligand (247 mg, 1.4 mmol) was recovered by evaporation of the acetone filtrate.) The extracted solid was then further extracted in 50 mL of toluene at reflux for 30 minutes to give a toluene-loaded sample that was free of bpene guests as determined by TGA. To make activation of the sample easier for gas adsorption measurements, the toluene was replaced by acetone by extraction in boiling acetone until TGA analysis showed complete exchange of toluene with acetone (1–2 hours). The adsorbed acetone was removed under vacuum at 90 °C overnight to give 1.22 g (3.0 mmol) of guest-free Ni(bpene)Ni(CN)$_4$. The formula weight of the product was verified from the residual weight of NiO after TGA in air to 550 °C.

Synchrotron X-ray diffraction experiment

The small crystal that we used (0.016 × 0.011 × 0.006 mm^3) has a thin-plate morphology. It was merohedrally twinned with a 5% of the twinned component. The crystal was mounted on the tip of a glass fiber with paratone oil and cooled down to 100 K with an Oxford Cryojet. An X-ray diffraction experiment was performed with a Bruker D8 diffractometer in the vertical mount with a APEX II CCD detector using double crystals technique with a Si(111) monochromator at 30 keV (λ = 0.41328 Å) at sector 15 (ChemMatCARS), Advanced Photon Sources (APS), Argonne National Laboratory. For the structure determination data, 1440 frames (0.5° φ scans) were collected at ω values of −180° and −150°. Data were processed with APEX2 suite software[13] for cell refinement and reduction. The structure was solved by the direct method and refined on F^2 (SHELXTL).[14] Non-hydrogen atoms were refined with anisotropic displacement parameters, and hydrogen atoms on carbons were placed in idealized positions (C–H = 0.95 Å).

Instrumentation

Isotherms were collected on a pressure–composition isotherm measurement system (Advanced Materials Corporation) for pressures up to 10 bars for CO_2. The instrument is designed on the basis of a conventional Sievert's apparatus. Prior to the measurements, the powder sample (~750 mg) was degassed under vacuum at 90 °C for 18 h. Thermogravimetric analyses were performed using a Mettler STARe TGA/DSC thermogravimetric analyzer. Samples (5–10 mg) were run in a 150 μL Pt pan using a temperature ramp of 15 °C min^{-1} under a dry air purge of 100 mL min^{-1} to temperatures > 550 °C. To determine the sample purity, the following calculations were performed using the TGA data. The expected formula weight of the guest-free Ni(bpene)Ni(CN)$_4$ compound is 403.6 g mol^{-1}. The complete oxidation in air will lead to 2 NiO units (149.39 g mol^{-1}) per Ni(bpene)Ni(CN)$_4$ formula unit. The ratio of the formula weight of nickel oxide to the formula weight of guest-free Ni(bpene)Ni(CN)$_4$ is 0.370. Dividing the mass of NiO obtained in the TGA run in air by the mass of corresponding guest-free Ni(bpene)Ni(CN)$_4$ should result in the same ratio of 0.370. On the TGA curve, the material was determined to be guest free at the plateau after guest solvents were lost.

Computational surface characterization

Computational methods were used to estimate the pore size distribution (PSD), to characterize the pore volume and surface area, and to obtain a visualization of the maximum space available for the uptake of CO_2 in the pore. The chosen technique of computing the PSD was the method of Gelb and Gubbins,[15] in which the local pore size at any given location in the material is equal to the diameter of the largest sphere that contains that point without overlapping the material framework. The value of the PSD at a particular pore diameter is then the fraction of the free volume with local pore size equal to that diameter. We first reconstructed the bpene material framework from the crystal structure data, identified the coordinates of each atom in the framework, and then drew a van der Waals exclusion sphere around each atom. (van der Waals radii were 1.63 Å for Ni, 1.09 Å for H, 1.70 Å for C, and 1.55 Å for N.)[16] The PSD was then numerically calculated *via* the voxel technique described by Palmer *et al.*[17] using cubic voxels with side length 0.1 Å or smaller. We computed the PSD for two cases, one in which the free bpene ligands are present and a second in which the free bpene ligands were removed from the pore channels. In both situations, all solvent molecules were evacuated. The pore volume and surface area were characterized by the so-called accessible volume and accessible surface area metrics, which were computed as described by Düren and coworkers.[18] The framework atoms were assigned the radii listed above and N_2 with assigned diameter of 3.681 Å was used as the probe gas. Use of N_2 with this diameter as the computational probe is expected to yield an accessible surface area that correlates well with the BET surface area measured by N_2 adsorption.[19]

Results and discussion

The selected data collection parameters and refinement results are listed in Table 1. Selected bond distances are given in Table S1 as ESI.†

Crystal structure analysis

In the following discussion, for simplicity, we refer to the sorbent as Ni(bpene)[Ni(CN)$_4$], which was found to adopt the 3-D Hofmann-type structure.[6] The molecular structure of the asymmetric unit with partial labeling is shown in Fig. 2, and complete labeling is given in Fig. S1, ESI.† The framework is based on the 2-D infinite layer-like tetracyanonickelate [Ni(CN)$_4$]$^{2-}$ planar complex.[20] Ni3 and Ni4 are each coordinated to four C atoms of the C≡N groups forming a square-planar geometry. The N ends of the C≡N ligand further coordinate to Ni1 and Ni2 which act as linear linkers between the tetracyanonickelate molecules. All C≡N groups are bridging, creating a 2-D square grid network (Fig. 3). The Ni1 and Ni2 ions are octahedrally surrounded by six N atoms, four from the C≡N units and the other two from two bpene ligands. The layers are pillared by the bpene ligands, which occupy the axial positions of the [NiN$_6$] octahedron. These bpene ligands further bridge together the 2-D Ni[Ni(CN)$_4$] sheets to form the 3-D pillared-layered structure as shown in Fig. 4a and 4b. In Fig. 4b, Ni1and Ni2 are shown to have an octahedral environment while Ni3 and Ni4 adopt a square-planar geometry. The bpene pillar ligands and the Ni[Ni(CN)$_4$] layers encase empty voids of parallelepiped shapes which are created

Table 1 Crystal data, data collection and structure refinement information for Ni(bpene)[Ni(CN)$_4$]·½bpene·DMSO·2H$_2$O[a]

Empirical formula:	
Determined	Ni(bpene)[Ni(CN)$_4$] $Ni_2N_7C_{24}H_{25}SO_3$
Expected	Ni(bpene)[Ni(CN)$_4$]·½bpene·DMSO·2H$_2$O $Ni_2N_6C_{16}H_{10}$
T/K	100
Diffractometer	Bruker Smart Apex II CCD
Wavelength (synchrotron)/Å	0.41328
Crystal size/mm^3	0.016 × 0.011 × 0.00
Crystal habit	Plate-like
Crystal system	Monoclinic
Space group	$P2_1/m$ (no. 11)
a/Å	13.5941(12)
b/Å	14.3621(12)
c/Å	14.2561(12)
β/°	96.14(1)
V/Å^3	2767.4(4)
Z	4
D_c/g cm^{-3}	1.46
F(000)/e	1248
Radiation source	Synchrotron
Total frames	1440
Frame size/pixels	512
Total measurement time/min	40
Data collection method	φ scans
θ range for data collection/°	0.84 to 20.00
Index ranges	$-22 \leqslant h \leqslant 20$ $-17 \leqslant k \leqslant 23$ $-23 \leqslant l \leqslant 21$
Reflections collected	13 373
Observed reflection, $I > 2\sigma(I)$	5064
Variation in check reflections/%	0
Absorption correction	Multi-scan SADABS[12]
Structure solution refinements	SHELXS-97[13]
Function minimized	$\Sigma w(F_o^2 - F_c^2)^2$
Data/restraints/parameters	13 373/593/449
Goodness-of-fit	0.928
Final R indices:	
R_1, $I > 4\sigma(I)$	0.0448
wR_2, all data	0.106
Extinction coefficient	0.0108(8)
Largest diff. peak and hole/e Å^{-3}	1.205 and −0.771

[a] $w = 1/[\sigma^2(F_o^2) + (0.03P)^2 + 0.00P]$, $P = [\max(F_o^2, 0) + 2F_o^2]/3$. $R_1 = \sum||F_o| - |F_c||/\sum|F_o|$, $wR_2 = [\sum w(F_o^2 - F_c^2)^2/\sum w(F_o^2)^2]^{1/2}$.

by the absence of bpene coordination to Ni3 and Ni4 of the square plane [Ni(CN)$_4$] building units. These void spaces provide pockets for the encapsulation of guest molecules.[5]

The chains that make up the 2-D Ni[Ni(CN)$_4$] sheets are arranged in a zig-zag manner (for example, deviations of bond angles from 180° are observed in the following: 174.7(2)° (C1–N1–Ni1), 176.4(2)° (N2–C2–Ni4), 173.0(2)° (C2–N2–Ni2), 171.4(2)° (C3–N3–Ni2), and 171.4(2)° (C4–N4–Ni1)). The bond distances of Ni–N and Ni–C within the 2-D sheet are all within the expected range (Table S1, ESI†). The Ni3 and Ni4 have a square-planar arrangement, and the mean Ni–C (1.860 Å) and C≡N (1.153 Å) bond lengths agree with the values reported for other tetracyanonickelate salts.[21] The Ni–N distances (ranging from 2.0168(13) Å to 2.099 (2) Å) are substantially longer than the Ni–C distances (1.856(2) Å to 1.865(2) Å), which also conform to the literature values.[22] The 6-coordination Ni are of high spin configuration because nitrogen is acting as a weak-field ligand. When the Ni atom only has 4-coordination (such as that in Ni(CN)$_2$),[23] the low-spin square-planar coordination of Ni^{2+} ions results in a contraction.

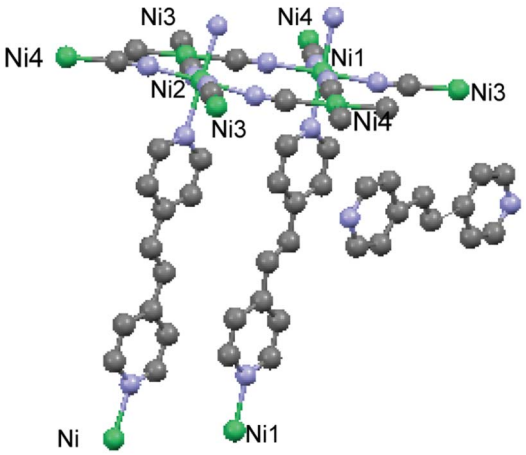

Fig. 2 A basic motif of the Ni(bpene)[Ni(CN)$_4$] molecules (not including solvents), with partial labeling scheme provided (green – Ni, blue – N, grey – C).

Positional disorder was observed with half of the coordinated bpene ligand molecules in the unit cell. Apparently there is sufficient space in the unit cell so these ligands have freedom to take on more than one configuration. In the bpene ligand, the ethylene moiety (C=C double bond) that connects the two pyridyl rings can have two conformations (Fig. S2, ESI†). We found that while the bpene molecule that is coordinated to Ni2 has an ordered configuration, the ligand that is coordinated to Ni1, however, has two variations (one configuration has an occupancy factor of 0.724(2) and the other version 0.276(2)). Both variants are planar and have the positions of the six-membered rings off set from each other (Fig. S2, ESI†); the conformations of the C=C bond linking between the two pyridine rings are in the opposite directions. Fig. 5a and 5b give two examples of the resolved disordered structure, featuring different conformations of the –C=C– groups.

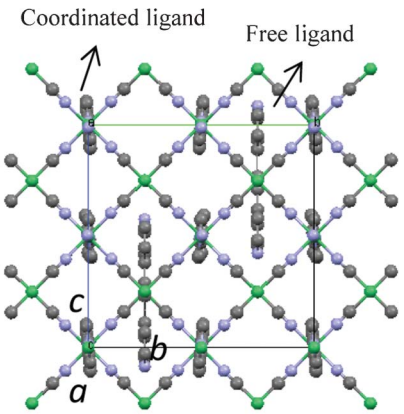

Fig. 3 2-D square grid network form by tetracyanonickelate molecules and the bridging C≡N group (green – Ni, blue – N, grey – C).

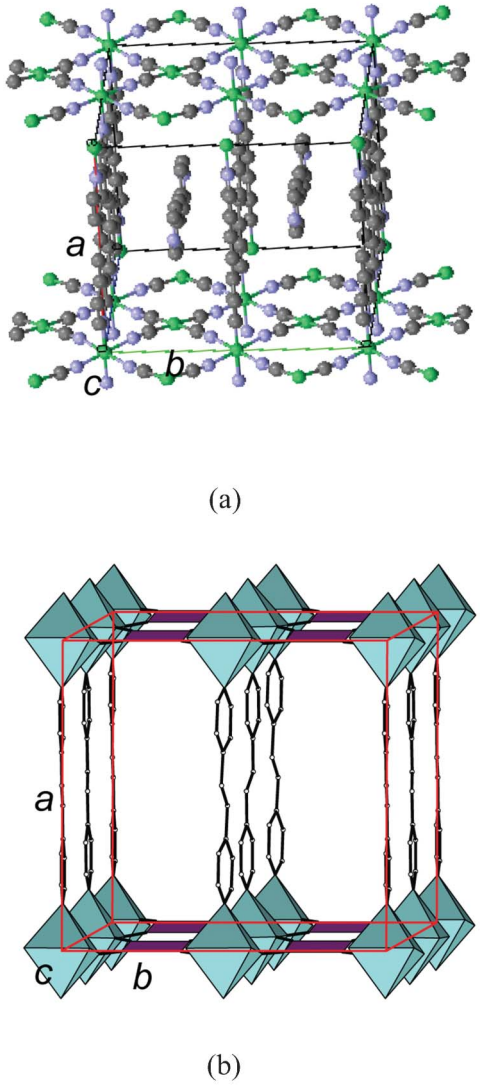

Fig. 4 (a) Framework structure of Ni(bpene)[Ni(CN)$_4$] showing the 2D nets connected by the bpene ligands to form a 3D network (green – Ni, blue – N, grey – C); (b) polyhedral view of the octahedral and square-planar coordination environments in Ni(bpene)[Ni(CN)$_4$].

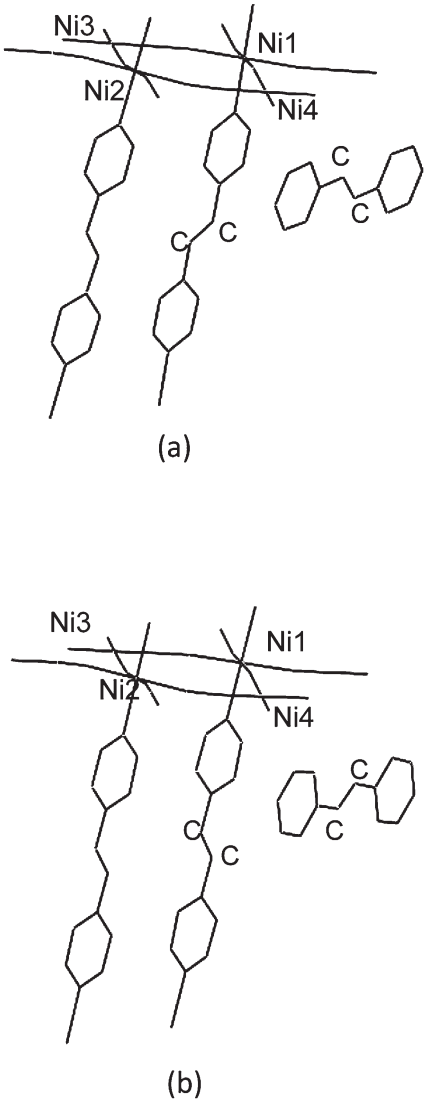

Fig. 5 (a) and (b) Structure of Ni(bpene)[Ni(CN)$_4$] illustrating examples of two possible arrangements of the free and coordinated bpene ligands.

It was interesting to observe that free bpene ligands that are not coordinated to any Ni atoms are also present in the cavities of the structure. A similar encapsulation of uncoordinated free bpene was recently reported in the structurally related spin crossover compound {Fe(bpene)[Pt(CN)$_4$]}·0.5(bpene)·H_2O.[10] The 'free ligands' are also disordered and lie on a crystallographic mirror plane. The two disordered versions are present in nearly equal amounts (occupancy of 0.268(1) *vs.* 0.232(1)). The two disordered variants of the free ligand are also related to each other *via* different conformation of the C=C double bond of the ethylene group. The two conformations of the –C=C– ethylene linkage is likely the driving force behind the disordered configurations of the ligand molecules. Since the disorder was observed with a data set collected at 100 K, it is expected that the disorder at room temperature will be more extensive. For example, the free ligands may even involve rotational disorder. The bond distances found in the coordinated and free ligand moieties (ordered and disordered) are all within the expected range (Table S1, ESI†).

Solvent molecules used as solvent of crystallization, such as water and DMSO, were also found inside the cavities (Fig. 6). There are two crystallographic independent groups of disordered DMSO molecules, each with ½ occupancy, located in the unit cell. The ''resolved'' disordered positions are also shown in Fig. 7a and 7b. Each disordered DMSO molecule is located near a mirror plane and therefore each molecule is superimposed with its own mirror image, giving rise to a total of 1 DMSO per formula unit. A total of 2 water molecules per formula unit were found disorderly distributed throughout the unit cell occupying 6 different sites; each site is associated with only between ¼ and ½ occupancy. Because of the disorder situation of the water molecules, hydrogen atoms of the water molecules were not located.

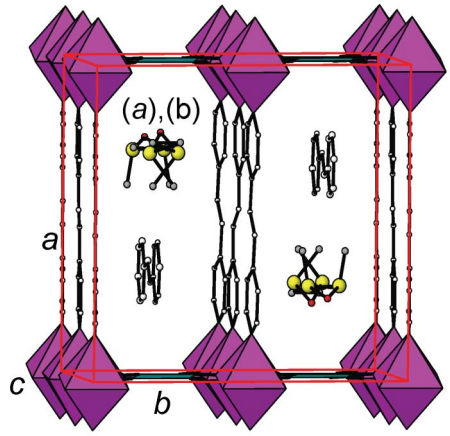

Fig. 6 A parallel view of the tunnel in Ni(bpene)[Ni(CN)$_4$]·½bpene·DMSO·2H$_2$O showing the entrapped free ligands, and disordered DMSO molecules (a) and (b).

The final empirical formula of the compound, reflecting the fact that additional DMSO and water solvent molecules, and free bpene ligands are captured inside the structure, can be written as Ni(L)[Ni(CN)$_4$]·½L·DMSO·2H$_2$O, (where L = 1,2-bis(4-pyridyl)ethylene), or $(C_{16}H_{10}N_6Ni_2)\cdot\frac{1}{2}(N_2C_{12}H_{10})\cdot(SC_2OH_6)\cdot 2H_2O$, resulting in $Ni_2N_7C_{24}H_{25}SO_3$. There are a total of 4 such formula units per unit cell, resulting in an estimated density of 1.46 g cm^{-3}.

Single crystals for Ni(bpene)[Ni(CN)$_4$] without the encapsulated guest molecules are notoriously difficult to grow for the purpose of structure determination because of the tendency of pore collapse. Using the current unit cell data, we were able to perform least-squares lattice refinements and index the X-ray diffraction pattern of the powder sample of Ni(bpene)[Ni(CN)$_4$]. Fig. S3, ESI† gives the diffraction pattern of Ni(bpene)[Ni(CN)$_4$] including selected representative indices. The lattice parameters of the powder sample without DMSO molecules were $P2_1/m$, a = 13.77(4) Å, b = 14.73(7) Å, c = 12.39(3) Å, β = 113.0(2)°, V = 2314.4 Å^3. While the lattice parameters of those of the current single crystal with inclusion of DMSO–water–bpene (a = 13.5941(12) Å, b = 14.3621(12) Å, c = 14.2561(12) Å, β = 96.141(2)°, V = 2767.4(4) Å^3) are similar, the β angles of the two monoclinic unit cells are substantially different. The β angle decreases from 113.0(2)° to 96.141(2)° with guest inclusion. As previously proposed by Culp *et al.*,[8] the schematics of the flexible crystal structure (α-phase) opening up the unit cell as the guests are included (β-phase) are shown in Fig. 8.[8] We plan to determine the structure of Ni(bpene)[Ni(CN)$_4$] using Rietveld refinements technique[24] on a powder sample to be collected at the APS powder diffraction facility.

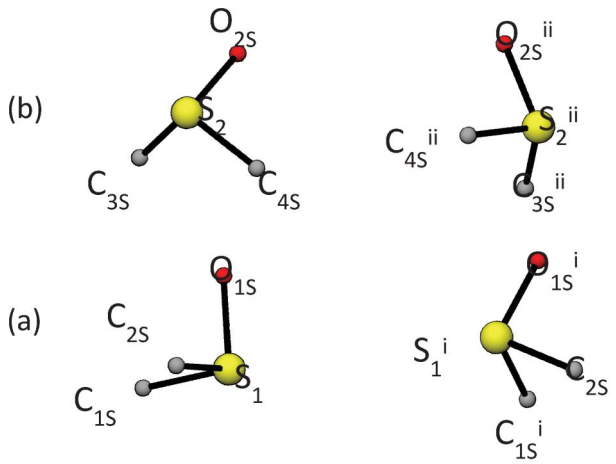

Fig. 7 (a) and (b) The ''resolved'' configurations of the disordered DMSO molecules with symmetry codes (a) x, 1/2 − y, z, (b) x, 3/2 − y, z.

Pore size distribution, pore volume, and surface area

Fig. 9a and 9b display a schematic representation of Ni(bpene)[Ni(CN)$_4$] (based on the crystal structure data given in this work) for two cases: (a) the free bpene ligands have been artificially removed and (b) the free bpene ligands are present. In both cases, van der Waals radii have been drawn about each constituent atom to indicate the approximate space taken up by the framework atoms. There is an unobstructed pore of approximate width 3.5 Å in both cases, though the free ligands significantly reduce the width of the pore in the direction perpendicular to the Ni(CN)$_4$ plane. Without the free bpene ligands, the free volume (that not occupied by the framework atoms) is approximately 61% of the total volume; the free volume fraction is reduced to 50% with the free ligands present. This corresponds to a 19% reduction in the free volume that could contain adsorbate molecules.

The pore size distribution in Fig. 10 was computed using the structure shown in Fig. 9a and 9b (with the free bpene ligands absent and present, respectively). For both cases, much of the free volume has local pore size less than 3 Å (58% and 34% with and without the free ligands, respectively) which is practically inaccessible to sorbates of any size. The main pore channel with diameter 3.5 Å is visible in the PSD for both cases, although larger pores (with non trivial contributions to the PSD) are present, most prominently the pore of local diameter 5.7 Å for case (a) without the free ligands. These larger pores are voids in the material where a relatively large sphere can reside, but that sphere could not pass through the 3.5 Å main aperture. Consequently, maximum uptake of a non-spherical sorbate may involve rotation or rearrangement of the sorbate after it passes through the main aperture to achieve

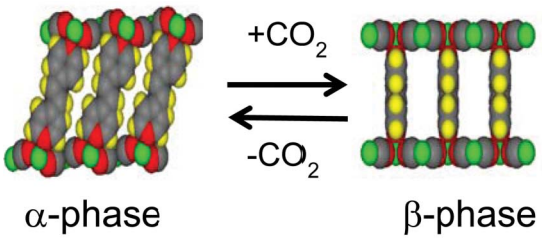

Fig. 8 Schematic drawing demonstrating the opening/collapsing (decreasing/increasing β angle) of the monoclinic unit cells of Ni(bpene)[Ni(CN)$_4$] as previously proposed by Culp *et al.*[8]

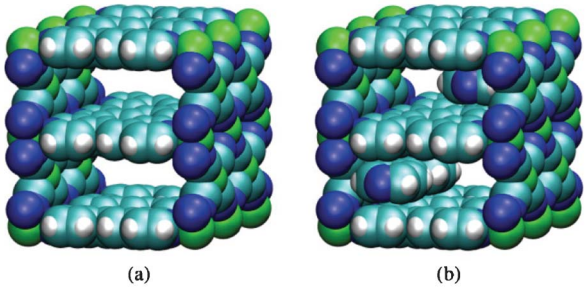

Fig. 9 Molecular structure of Ni(bpene)[Ni(CN)$_4$] (without solvent), with van der Waals exclusion volume of all atoms[16] shown by colored spheres. Atomic positions were obtained *via* the crystallographic information from this work. (a) Structure without free bpene ligands. (b) Structure with free bpene ligands. Color codes for atoms: cyan, C; blue, N; white, H; green, Ni.

higher packing. Inclusion of the free bpene ligand in the pore structure also alters the PSD by eliminating some of the free space with local pore size 3.9 Å and greater and completely eliminates free space with pore size greater than 5.1 Å. Examination of these two PSDs highlights the reduction in free volume and in the reduction in local pore size of that free volume, which are indicative of reduced adsorption capacity due to the presence of the free ligands.

The accessible surface areas for the structures shown in Fig. 9a and 9b were computed using N_2 as the probe gas. For Fig. 9a, the structure without free ligands, was found to have an accessible surface area of 1731.20 ± 3.72 $m^2\ g^{-1}$ (uncertainty bounds based on a 95% confidence interval *t*-test). Addition of the free ligands (Fig. 9b) reduces the accessible surface area to 411.65 ± 1.13 $m^2\ g^{-1}$. With the same N_2 probe, the accessible pore volume (*e.g.*, the pore

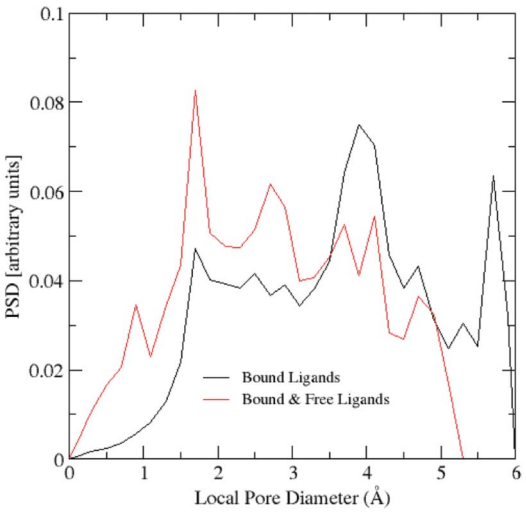

Fig. 10 Pore Size Distribution (PSD) of Ni(bpene)[Ni(CN)$_4$] as a function of local pore diameter, as calculated by the method of Gelb and Gubbins[15] and described in the text. The solid black line is the PSD for the material with only the bound bpene ligands (*i.e.*, the free ligands in the pore channels have been removed) and the solid red line is the PSD for the material with all bpene ligands present.

volume available to N_2 centers[18]) for the structure in Fig. 9a was computed as 0.05683 ± 0.00012 $cm^3\ g^{-1}$. That for Fig. 9b was 0.00990 ± 0.00006 $cm^3\ g^{-1}$. Both of the accessible geometry metrics highlight the pore congestion associated with the structures that include free bpene ligands.[19]

Synthetic techniques

A technique that we have found to be quite versatile for crystallization of Ni(L)[Ni(CN)$_4$] compounds is a modification of a procedure originally used by Cernak *et al.* to prepare crystalline 1-D [Ni(CN)$_4$] containing chain compounds.[25] The approach involves the use of NH_3 as a blocking ligand since a sufficient concentration of NH_3 will prevent the formation of Ni–CN–Ni and Ni–L–Ni bridges required for polymerization of the coordination polymer. If the reaction mixture is contained in an open flask, the NH_3 will outgas from the solution. Once the concentration of NH_3 drops below a threshold level, assembly of the Ni(L)[Ni(CN)$_4$] material will commence. Using a H_2O–DMSO mixture as the solvent and a reaction temperature of ~90 °C provided the necessary combination of NH_3 out gassing rate and oligomer solubility to produce the targeted 3-D polymeric structure. A good crop of crystals can typically be obtained in 24 h to 48 h. The technique has been found to be adaptable to various organic bridging ligands (L) and has provided several crystalline samples that are currently under analysis in our laboratory.

A larger scale synthesis (to conveniently produce the quantities of polycrystalline material required for gas adsorption measurements) was developed by modifying the synthesis used to prepare the single crystal sample. The temperature of the reaction was lowered to room temperature and an aspirator was used to expedite the outgassing of NH_3 from the reaction mixture. The reaction is complete in about 90 minutes and the guest-loaded material can be activated by sequential extraction with refluxing acetone, then refluxing toluene, then again in refluxing acetone to get a sample that can be evacuated at a relatively mild temperature of 90 °C.

The effectiveness of the extraction method can be followed using thermogravimetric analysis (TGA). When ran in air, the final decomposition product is nickel oxide (NiO) which gives a convenient method of calculating the formula weights of the material throughout the temperature ramp. The data in Fig. 11 compare the TGA of the single crystal material (A) and the polycrystalline sample through various stages of extraction and activation (B–E). The TGA for the single crystal material (trace A) shows weight loss steps corresponding to the loss of H_2O and DMSO guests prior to a plateau region which ends with combustion of the sample. The mass loss of 19 wt% agrees well with that expected for the loss of $2H_2O$ + DMSO from the Ni(bpene)[Ni(CN)$_4$]·½bpene·DMSO·$2H_2O$ empirical formula that was determined from the X-ray structure determination. Furthermore, the formula weight of the compound in the plateau region is calculated to be 494.7 from the weight of residual NiO which matches that expected for Ni(bpene)[Ni(CN)$_4$]·½bpene. For the polycrystalline sample, the TGA trace (B) is different in that it shows a continued weight loss up to the decomposition point, likely due to the presence of additional bpene ligands or guests. However, after extractions with acetone and toluene, the TGA trace (C) shows

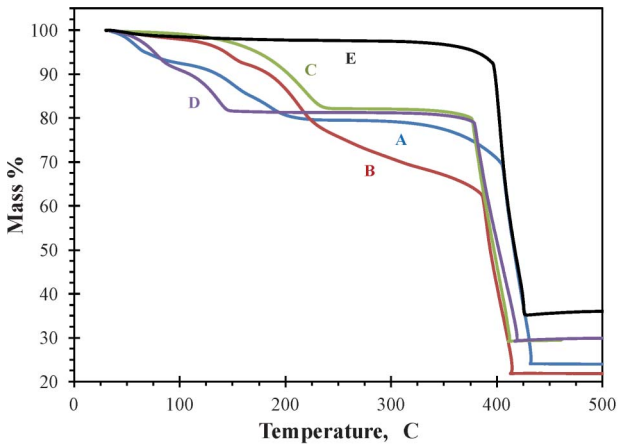

Fig. 11 Normalized TGA curves measured in air for various [Ni(bpene)Ni(CN)$_4$-(guests)] samples. (A) Single crystals with guest H_2O, DMSO, and bpene; (B) polycrystalline sample after vacuum drying at RT for 18 h with guests DMSO and bpene; (C) air-dried polycrystalline sample after extraction with acetone, then toluene; (D) polycrystalline sample C after further extraction with acetone; (E) polycrystalline sample D after vacuum drying at 90 °C overnight.

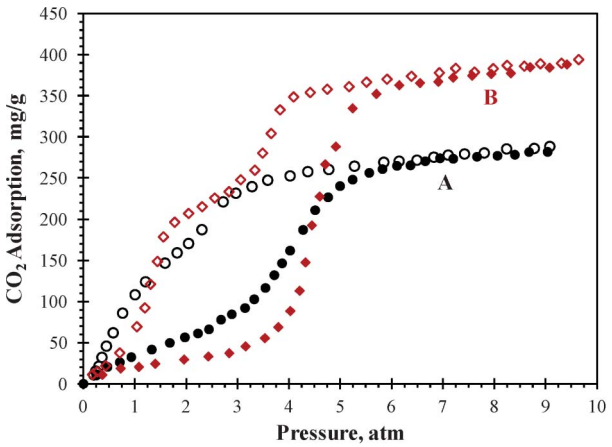

Fig. 12 Comparison of CO_2 adsorption (solid symbols)–desorption (open symbols) isotherms measured at 0 °C for (A) Ni(bpene)Ni(CN)$_4$ powder sample prepared[8] and (B) Ni(bpene)Ni(CN)$_4$ polycrystalline sample prepared by the method reported herein.

a single step weight loss of 18% which agrees well with that expected for Ni(bpene)[Ni(CN)$_4$] toluene. Extraction of the toluene-loaded materials with acetone produces the material with trace (D) that shows a two-step weight loss at a lower temperature than that of Ni(bpene)[Ni(CN)$_4$]·toluene, indicating complete guest exchange of toluene for acetone and no evidence of guest bpene. The formula weight calculated for the plateau region is 406.4 g mol^{-1} which agrees nicely with the expected formula weight of guest-free Ni(bpene)[Ni(CN)$_4$] of 403.7 g mol^{-1}. The two steps observed in the weight loss of acetone agrees well with the two site adsorption mechanism previously observed for adsorption of acetone in the powder sample of Ni(bpene)Ni(CN)$_4$.[8]

CO_2 adsorption

The effectiveness of the new synthetic technique for the preparation of polycrystalline Ni(bpene)[Ni(CN)$_4$] is further exemplified by the 40% enhancement in adsorption capacity of the material as compared to the originally reported powder sample which was made by an intercalation reaction of the bpene linker into preformed polymeric Ni[Ni(CN)$_4$]. While the overall isotherm behavior of the two materials shown in Fig. 12 is similar in that both show isotherm inflections at similar pressures consistent with structurally dynamic behavior as schematically depicted in Fig. 8, the two steps in the desorption isotherm of the newly prepared polycrystalline material are more clearly defined. The two step loss of acetone in the TGA analysis shown in trace D of Fig. 11 is quite similar to the two step desorption of CO_2 clearly observed in the isotherms shown in Fig. 12 and indicates an intermediate structural phase between the fully guest-loaded and fully guest-free states.

The fully CO_2-loaded phase, corresponding to a loading of approximately 3.6 CO_2 molecules per Ni(bpene)[Ni(CN)$_4$] formula unit, or 14.4 CO_2 per unit cell, transitions to the intermediate phase after a loss of approximately 40% of the saturated loading of CO_2. Using a very rough estimate of a 4.2 Å diameter sphere (larger than C at 3.4 Å diameter and smaller than the major axis of 5.36 Å of CO_2), and ignoring CO_2 mutual overlapping, the free volume with local pore size greater than 4.2 Å could accommodate 16.3 CO_2 per unit cell. This value appears to exceed the experimental estimate for CO_2 capacity, but such an overestimation is expected since mutual CO_2 overlap was ignored.

Based on the propensity of the Ni(bpene)[Ni(CN)$_4$] material to incorporate guest bpene molecules, it is likely that the decreased capacity of the originally reported powder sample is the result of an incomplete extraction of guests during the activation procedure. This conclusion is supported by powder diffraction analyses of the ''guest-free'' phases of the previously reported material and the new material reported herein. When the low angle diffraction regions for the two compounds are compared in Fig. 13, it is clear that the newly prepared material undergoes a more complete transition to the collapsed phase with a smaller interlayer *d*-spacing. The presence of a small amount of residual guests could certainly interfere with the complete collapse of the previous material to the guest-free phase. The difficulty of guest extraction and activation of porous materials has previously been elegantly investigated for other MOFs where dramatic increases in CO_2 capacities were reported when super critical CO_2 was used as an extractant.[26] In the report, the authors hypothesized that ''thermal evacuation of solvent causes the collapse of inter-particle mesopores. Misalignment of micropores at particle–particle boundaries then inhibits access by gas molecules to internal (microporous) surfaces.''[26] A similar mechanism could also be responsible here for the lower uptake of CO_2 in the original powder sample.

Conclusions and future work

A new synthetic technique has been developed for the synthesis of crystalline 3-D Hofmann compounds which uses

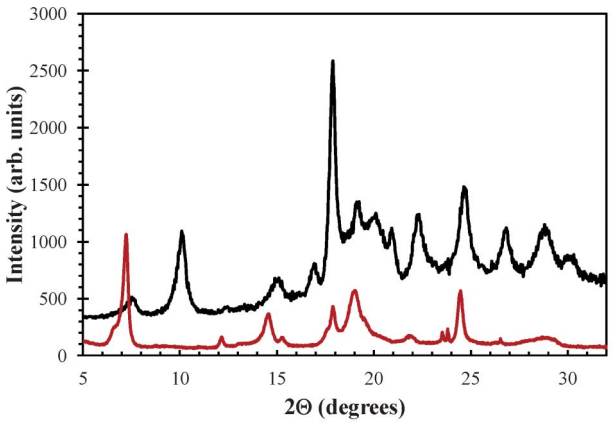

Fig. 13 Comparison of powder XRD patterns of evacuated Ni(bpene)[Ni(CN)$_4$] for a sample prepared by the current synthetic method (black, top trace; for *hkl* indexes, see Fig. S3, ESI†) with that obtained by the previously reported method (red, lower trace).[8]

slow outgassing of NH_3 from a solution of Ni(II), $[Ni(CN)_4]^{2-}$, and bpene in an NH_3, H_2O and DMSO mixture. At elevated temperature, slow growth of the product produces single crystals of Ni(bpene)[Ni(CN)$_4$]·½bpene·DMSO·2H_2O of sufficient quality for X-ray structural analysis. The structure consists of a pillared-layer motif where layers consist of cyanide bridged Ni–(CN)$_4$–Ni networks which are pillared into an extended 3-D structure by bridging bpene ligands. The absence of coordinated ligands to the square-planar [Ni(CN)$_4$] sites produce pores occupied by solvent and guest bpene molecules. When a similar reaction mixture is reacted at room temperature under reduced pressure, a polycrystalline product is produced. Extraction of the polycrystalline product with acetone and toluene followed by evacuation of guest solvents gave a guest-free material Ni(bpene)[Ni(CN)$_4$] with an improved CO_2 capacity approximately 40% higher than originally reported for the powder sample produced by a different synthetic technique.[8] However, the structural flexibility of Ni(bpene)[Ni(CN)$_4$] originally proposed based on analysis of the powder sample was confirmed with the newly synthesized polycrystalline material.

Analysis of the guest-free small pore phase of Ni(bpene)[Ni(CN)$_4$] is currently under investigation in our laboratory using powder diffraction analysis. Preliminary results confirm the originally proposed hypothesis that the structural flexibility in the material is a result of a shift in the β angle of the unit cell as the material transitions between the guest-free and guest-loaded phases.[8] Results of single crystal data further our understanding of *in situ* experiments concerning adsorption of CO_2 in the cavities of the bpene sample, as well as to elucidate the detailed adsorption mechanism of this fascinating compound for carbon mitigation applications. Further research is ongoing in our laboratories to prepare and characterize novel 2-D and 3-D open frameworks using tetracyanonickelates as building blocks, and to explore their adsorption properties.

Acknowledgements

This technical effort was performed in support of the National Energy Technology's ongoing research in CO_2 capture under the RES contract DE-FE0004000. The authors gratefully acknowledge ChemMatCARS Sector 15 which is principally supported by the National Science Foundation/Department of Energy under grant number NSF/CHE-0822838. Use of the Advanced Photon Source was supported by the U. S. Department of Energy, Office of Science, Office of Basic Energy Sciences, under Contract No. DE-AC02-06CH11357.

References

1 (*a*) S. M. Benson and F. M. Orr, *MRS Bull.*, 2008, **33**, 303; (*b*) M. L. Green, L. Espinal, E. Traversa and E. J. Amis, *MRS Bull.*, 2012, **37**, 303.
2 (*a*) S. R. Batten, N. R. Champness, X.-M. Chen, J. Garcia-Martinez, S. Kitagawa, L. Öhrström, M. O'Keeffe, M. P. Suh and J. Reedijk, *CrystEngComm*, 2012, **14**, 3001; (*b*) K. Biradha, A. Ramanan and J. J. Vittal, *Cryst. Growth Des.*, 2009, **9**, 2969.
3 (*a*) J. R. Li, J. Sculley and H. C. Zhou, *Chem. Rev.*, 2012, **112**, 869; (*b*) S. T. Meek, J. A. Greathouse and M. D. Allendorf, *Adv. Mater.*, 2011, **23**, 249; (*c*) H. C. Zhou, J. R. Long and O. M. Yaghi, *Chem. Rev.*, 2012, **112**, 673.
4 (*a*) G. Férey and C. Serre, *Chem. Soc. Rev.*, 2009, **38**, 1380; (*b*) L. Hamon, P. L. Llewellyn, T. Devic, A. Ghoufi, G. Clet, V. Guillerm, G. D. Pirngruber, G. Maurin, C. Serre, G. Driver, W. van Beek, E. Jolimaître, A. Vimont, M. Daturi and G. Férey, *J. Am. Chem. Soc.*, 2009, **131**, 17490; (*c*) S. Bureekaew, S. Shimomura and S. Kitagawa, *Sci. Technol. Adv. Mater.*, 2008, **9**, 014108.
5 (*a*) C. Y. Gao, S. X. Liu, L. H. Xie, Y. H. Ren, J. F. Cao and C. Y. Sun, *CrystEngComm*, 2007, **9**, 545; (*b*) R. Kitaura, K. Fujimoto, S. Noro, M. Kondo and S. Kitagawa, *Angew. Chem., Int. Ed.*, 2002, **41**, 133; (*c*) T. K. Maji, K. Uemura, H.-C. Chang, R. Matsuda and S. Kitagawa, *Angew. Chem., Int. Ed.*, 2004, **43**, 3269; (*d*) P. Song, B. Liu, Y. Li, J. Yang, Z. Wang and X. Li, *CrystEngComm*, 2012, **14**, 2296; (*e*) X. F. Wang, Y. Wang, Y. B. Zhang, W. Xue, J. P. Zhang and X. M. Chen, *Chem. Commun.*, 2012, **48**, 133.
6 K. A. Hofmann and F. Küspert, *Z. Anorg. Chem.*, 1897, **15**, 204.
7 (*a*) T. Iwamoto, *J. Inclusion Phenom. Mol. Recognit. Chem.*, 1996, **24**, 61; (*b*) X. Chen, H. Zhou, Y.-Y. Chena and A.-H. Yuan, *CrystEngComm*, 2011, **13**, 5666.
8 (*a*) J. T. Culp, M. R. Smith, E. Bittner and B. Bockrath, *J. Am. Chem. Soc.*, 2008, **130**, 12427; (*b*) J. T. Culp, C. Madden, K. Kauffman, F. Shi and C. Matranga, *Inorg. Chem.*, 2013, **52**, 4205.
9 J. T. Culp, S. Natesakhawat, M. R. Smith, E. Bittner, C. S. Matranga and B. Bockrath, *J. Phys. Chem.*, 2008, **C112**, 7079.
10 F. J. Muñoz-Lara, A. B. Gaspar, M. C. Muñoz, M. Arai, S. Jitagawa, M. Ohba and J. A. Real, *Chem.–Eur. J.*, 2012, **18**, 8013–8018.
11 (*a*) V. Niel, J. M. Martinez-Agudo, M. C. Munoz, A. B. Gaspar and J. A. Real, *Inorg. Chem.*, 2001, **40**, 3838; (*b*) C. Bartual-Murgui, L. Salmon, A. Akou, N. A. Ortega-Villar, H. J. Shepherd,

M. C. Muñoz, G. Molnár, J. A. Real and A. Bousseksou, *Chem.–Eur. J.*, 2012, **18**, 507; (*c*) P. D. Southon, L. Liu, E. A. Fellows, D. J. Price, G. J. Halder, K. W. Chapman, B. Moubaraki, K. S. Murray, J. F. Létard and C. J. Kepert, *J. Am. Chem. Soc.*, 2009, **131**, 10998.

12 Certain trade names and company products are mentioned in the text or identified in illustrations in order to adequately specify the experimental procedures and equipment used. In no case does such identification imply recommendation or endorsement by the National Institute of Standards and Technology.

13 APEX2 (2009.11-0), *Program for Bruker CCD X-ray Diffractometer control*, Bruker AXS Inc., Madison, WI, 2009.

14 G. M. Sheldrick, SHELXTL, version 6.14, *Program for Solution and Refinement of Crystal Structures*, Universität Göttingen, Germany, 2000.

15 L. D. Gelb and K. E. Gubbins, *Langmuir*, 1999, **15**(2), 305–308.

16 (*a*) A. Bondi, van der Waals Volumes and Radii, *J. Phys. Chem.*, 1964, **68**(3), 441–451; (*b*) R. S. Rowland and R. Taylor, *J. Phys. Chem.*, 1996, **100**(18), 7384–7391.

17 J. C. Palmer, J. D. Moore, J. K. Brennan and K. E. Gubbins, *J. Phys. Chem. Lett.*, 2011, **2**(3), 165–169.

18 (*a*) H. Frost, T. Düren and R. Q. Snurr, *J. Phys. Chem. B*, 2006, **110**, 9565; (*b*) T. Düren, F. Millange, G. Férey, K. S. Walton and R. Q. Snurr, *J. Phys. Chem. C*, 2007, **111**, 15350.

19 K. S. Walton and R. Q. Snurr, *J. Am. Chem. Soc.*, 2007, **129**, 8552.

20 S. Nishikiori, T. Hasegawa and T. Iwamoto, *J. Inclusion Phenom.*, 1997, **11**, 137.

21 (*a*) J. Černák and J. Lipkowski, *Monatsh. Chem.*, 1999, **130**, 1195; (*b*) T. Miyoshi, T. Iwamoto and Y. N. Sasaki, *Inorg. Chim. Acta*, 1973, **7**, 97–101; (*c*) T. Akitsu and Y. Einaga, *Inorg. Chem.*, 2006, **45**, 9826–9833; (*d*) M. Broring, S. Prikhodovski, C. D. Brandt and E. C. Tejero, *Chem.–Eur. J.*, 2007, **13**, 396–406.

22 (*a*) G. S. Kürkçüoğlu, O. Z. Yeşilel, I. Kavlak and O. Büyükgüngör, *Struct.*.

23 S. J. Hibble, A. M. Chippindale, A. H. Pohl and A. C. Hannon, *Angew. Chem., Int. Ed.*, 2007, **46**, 7116–7118.

24 A. C. Larson and R. B. von Dreele, *GSAS – General Structure Analysis System, US Government contract (W-7405-ENG-36) by the Los Alamos National laboratory, which is operated by the University of California for the U. S. Department of Energy*, 1992.

25 (*a*) J. Černák and K. A. Abboud, *Acta Crystallogr., Sect. C: Cryst. Struct. Commun.*, 2000, **56**, 783; (*b*) J..

26 A. P. Nelson, *et al.* Supercritical processing as a route to high internal surface areas and permanent microporosity in metal–organic frame-work materials, *J. Am. Chem. Soc.*, 2009, **131**, 458.